Optics Letters

Linear control of light scattering with multiple coherent waves excitation

Jeng Yi Lee,[1,2,6] Yueh-Heng Chung,[3] Andrey E. Miroshnichenko,[4,7] and Ray-Kuang Lee[3,5,8]

[1]Department of Applied Science, National Taitung University, Taitung 950, Taiwan
[2]Department of Opto-Electronic Engineering, National Dong Hwa University, Hualien 974, Taiwan
[3]Institute of Photonics Technologies, National Tsing Hua University, Hsinchu 300, Taiwan
[4]School of Engineering and Information Technology, University of New South Wales, Canberra ACT 2600, Australia
[5]Physics Division, National Center of Theoretical Sciences, Hsinchu 300, Taiwan
[6]e-mail: jengyilee@gms.ndhu.edu.tw
[7]e-mail: andrey.miroshnichenko@unsw.edu.au
[8]e-mail: rklee@ee.nthu.edu.tw

Received 9 August 2019; revised 3 September 2019; accepted 10 September 2019; posted 25 September 2019 (Doc. ID 375081); published 28 October 2019

With the wave interferometric approach, we study how extrinsically coherent waves excitation can dramatically alter the overall scattering properties, resulting in tailoring the energy assignment between radiation and dissipation, as well as filtering multipolar resonances. As an illustration, we consider cylindrical passive systems encountered by arbitrary configurations of incident waves with various illuminating directions, phases, and intensities. With formulas for dissipation and radiation powers, we demonstrate that a coherent superposition of incident waves extrinsically interferes with the targeted channels in a desirable way. Moreover, the interferometric results can be irrespective of inherent system properties such as size, material, and structure. Our approach paves a non-invasive solution to manipulate wave–obstacle interaction at will.

https://doi.org/10.1364/OL.44.005310

Scattering coefficients contain the complete information in light–obstacle interaction, including their multipolar resonances, energy distribution, radiation polarization, etc. [1–3]. A standard way to achieve the targeted scattering is to seek proper system configurations, with available materials embedded. For example, in the subwavelength dimension, the magnetic metaatom [4–6], invisible cloaking [7,8], superdirective antenna [9], perfect absorption object [10,11], Kerker scattering [12,13], anapole [14], and superscattering [15] are demonstrated.

Recently, it was shown that under structured illumination, inaccessible modes, which are not observed in conventional illumination, could be excited [16]. With a designed beam excitation, we can also suppress the dominant electric dipole (ED), and enhance the weaker magnetic response, resulting in asymmetrical Kerker effects [17]. These local electromagnetic responses offer opportunities for locating a sub-angstrom dimension in the spatial variation of phase and intensity [18,19]. Now, in addition to directly solving a given setting of structures and materials, the wave interferometric mechanism could also lead to peculiar functionalities for controlling light scattering.

Nevertheless, a generalized approach to provide details for multipolar resonance control is still missing. In this Letter, we derive formulas for the scattering and absorption powers in cylindrical systems, which are encountered by an arbitrary setting of coherent waves excitation. In particular, we reveal an interfering factor constituted by the linear superposition of excitation waves. This interfering factor responds to the manipulation of overall light scattering response, which not only modulates the resulting scattering channels but also affects the scattering distribution and dissipation energy outside and inside the scatterer, respectively. As a demonstration, we implement a set of impinging coherent waves to turn off or switch on the target channels, i.e., for both scattering radiation and dissipation energy. Moreover, to achieve the same scattering response, more than one solution can be found, which allows us to have the same scattering consequences by different irradiation settings. The results obtained by our methodology pave a useful non-invasive way to manipulate light scattering in desired ways.

Here, we consider a scatterer with cylindrical symmetry, which is illuminated by a monochromatic TM wave, i.e., the polarized magnetic field is along the z axis. The radius of our cylindrical object is denoted as a. The time evolution of the wave is chosen as $e^{-i\omega t}$, with the angular frequency ω, while the direction of propagation is on the $x-y$ plane with an angle Φ_1 with respect to the x axis. With the partial wave expansion, the corresponding magnetic field of our incident wave can be decomposed into a coherent sum of cylindrical waves, i.e., Jacobi–Anger expansion [20]: $\vec{H}_{in}^{(1)}(\theta, r) = \hat{z}\sum_{n=-\infty}^{\infty} i^n e^{in\theta - in\Phi_1} H_1 J_n(k_0 r)$. Here, J_n is a Bessel function, k_0 is the environmental wavenumber, and H_1 denotes the complex amplitude of an incident magnetic wave. Then, the associated scattered wave can be expressed as $\vec{H}_{\text{scat}}^{(1)} = \hat{z}\sum_{n=-\infty}^{\infty} i^n e^{in\theta - in\Phi_1} H_1 a_n^{\text{TM}} H_n^{(1)}(k_0 r)$, with the Hankel function of the first kind $H_n^{(1)}$, representing the out-going wave,

and the complex scattering coefficient a_n^{TM}, which is determined by boundary conditions. In this convergent series, each term represents a unique scattering multipolar channel: $n = 0$ for the magnetic dipole (MD), $n = \pm 1$ for the ED, and $n = \pm 2$ for the electric quadrupole (EQ). The corresponding electric field can be found by using the Maxwell–Ampére equation.

Now, for multiple coherent waves excitation, as illustrated in Fig. 1(a), the resulting incident waves can be obtained based on a linear superposition:

$$\begin{aligned}\vec{H}_{in} &= \vec{H}_{in}^{(1)} + \vec{H}_{in}^{(2)} + \cdots + \vec{H}_{in}^{(N)} \\ &= \hat{z}\sum_{n=-\infty}^{\infty} i^n e^{in\theta} \sum_{m=1}^{m=N} e^{-in\Phi_m} H_m J_n(k_0 r). \end{aligned} \tag{1}$$

Here, we assume that there are N incident waves. Each of them has its own propagation direction Φ_m and the complex amplitude H_m. As a consequence, the corresponding total scattering wave has the following form:

$$\begin{aligned}\vec{H}_{\mathrm{scat}} &= \vec{H}_{\mathrm{scat}}^{(1)} + \vec{H}_{\mathrm{scat}}^{(2)} + \cdots + \vec{H}_{\mathrm{scat}}^{(N)} \\ &= \hat{z}\sum_{n=-\infty}^{\infty} i^n e^{in\theta} H_n^{\mathrm{inf}} a_n^{\mathrm{TM}} H_n^{(1)}(k_0 r), \end{aligned} \tag{2}$$

with the introduction of an interfering factor involving all the excitation, i.e.,

$$H_n^{\mathrm{inf}} = \sum_{m=1}^{m=N} e^{-in\Phi_m} H_m. \tag{3}$$

Note that this interfering factor also depends on the channel index n, giving different effects on different channels. In the following, we will illustrate that this interfering factor, H_n^{inf}, plays a crucial role in the interferometric effect, resulting in tuning the scattering field for outside and internal field for inside the scatterer.

To obtain the total scattering and absorption powers, we apply the Poynting power vectors, as well as asymptotic analysis, to calculate the net power integrated over a closed area. The corresponding absorption and scattering powers for multiple coherent waves excitation can be found as

$$\begin{aligned} P_{\mathrm{abs}}^{\mathrm{TM}} &= -\frac{2}{k_0}\sqrt{\frac{\mu_0}{\epsilon_0}} \sum_{n=-\infty}^{n=\infty} |H_n^{\mathrm{inf}}|^2 \{\mathrm{Re}[a_n^{\mathrm{TM}}] + |a_n^{\mathrm{TM}}|^2\}, \\ P_{\mathrm{scat}}^{\mathrm{TM}} &= \frac{2}{k_0}\sqrt{\frac{\mu_0}{\epsilon_0}} \sum_{n=-\infty}^{n=\infty} |H_n^{\mathrm{inf}}|^2 |a_n^{\mathrm{TM}}|^2. \end{aligned} \tag{4}$$

Here, ϵ_0 and μ_0 are environmental permittivity and permeability, respectively. We want to remark that, unlike the scenario with conventional (single) illumination, the interfering factor H_n^{inf} provides an extrinsic way to control the scattering states.

Without loss of generality, we consider a single-layer cylinder embedded by isotropic and homogeneous electromagnetic material, as an example. Nevertheless, our methodology can be easily applied to other structures. We note that in subwavelength dimension $k_0 a < 1$, the primary channels to extrinsic scattering are usually dominant from $n = -2$ to $n = 2$. In the following, we therefore embed five beams to achieve the results. As illustrated in Fig. 1(b), we denote the corresponding complex amplitudes as $[H_1, H_2, H_3, H_4, H_5]$, illuminating from different impinging angles, $[\Phi_1, \Phi_2, \Phi_3, \Phi_4, \Phi_5]$. The corresponding interfering factor has the form $H_n^{\mathrm{inf}} = H_1 e^{-in\Phi_1} + H_2 e^{-in\Phi_2} + H_3 e^{-in\Phi_3} + H_4 e^{-in\Phi_4} + H_5 e^{-in\Phi_5}$. For each excitation wave, there are three degrees of freedom: direction of illumination Φ_i, intensity $|H_i|^2$, and its phase $\mathrm{Arg}[H_i]$. Then, for the lowest five channels (from $n = -2$ to $n = 2$), one can write down the incident waves configuration for interfering factors in a matrix form:

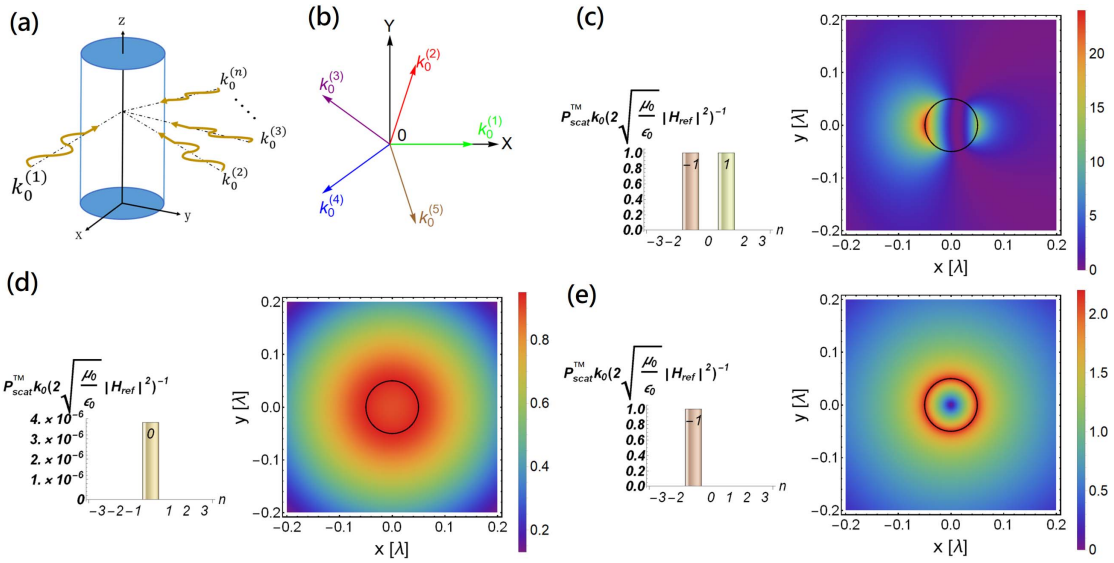

Fig. 1. (a) Illustration of our scattering system with multiple coherent waves excitation. (b) Example of five incident TM waves to the scatterer. As a comparison, a single wave excitation along x axis is shown in (c), with the normalized scattering powers, equivalent to $|a_n^{\mathrm{TM}}|^2$ (left panel) and the intensity of total magnetic field (right panel). Results for multiple (five) coherent waves excitation is shown in (d), with the normalized scattering powers (left panel) and the intensity of total magnetic field (right panel). Results from a different set of wave amplitudes, but with the same arrangement of illumination directions, are shown in (e), revealing the $n = -1$ ED pattern. Note that all the field plots are depicted in units of $|H_{\mathrm{ref}}|^2$.

$$\begin{bmatrix} e^{i2\Phi_1} & e^{i2\Phi_2} & e^{i2\Phi_3} & e^{i2\Phi_4} & e^{i2\Phi_5} \\ e^{i\Phi_1} & e^{i\Phi_2} & e^{i\Phi_3} & e^{i\Phi_4} & e^{i\Phi_5} \\ 1 & 1 & 1 & 1 & 1 \\ e^{-i\Phi_1} & e^{-i\Phi_2} & e^{-i\Phi_3} & e^{-i\Phi_4} & e^{-i\Phi_5} \\ e^{-i2\Phi_1} & e^{-i2\Phi_2} & e^{-i2\Phi_3} & e^{-i2\Phi_4} & e^{-i2\Phi_5} \end{bmatrix} \begin{bmatrix} H_1 \\ H_2 \\ H_3 \\ H_4 \\ H_5 \end{bmatrix} = \begin{bmatrix} H_{-2}^{\text{inf}} \\ H_{-1}^{\text{inf}} \\ H_0^{\text{inf}} \\ H_1^{\text{inf}} \\ H_2^{\text{inf}} \end{bmatrix}. \tag{5}$$

The obtained matrix shown in Eq. (5) implies that when we assign the desired interfering factors and illumination directions, the corresponding five incident waves $[H_1, H_2, H_3, H_4, H_5]$ can be found.

As an illustration, as depicted in Fig. 1(b), we choose the irradiation system with $[\Phi_1 = 0, \Phi_2 = 2\pi/5, \Phi_3 = 4\pi/5, \Phi_4 = 6\pi/5, \Phi_5 = 8\pi/5]$. A lossless scatterer with ED resonance, i.e., $|a_1^{\text{TM}}| = |a_{-1}^{\text{TM}}| = 1$, and with permittivity $\epsilon_1 = -1.156$ and permeability $\mu_1 = 1$, is considered as our studied system. The radius of the system is $a = 0.05\lambda$. As a comparison to conventional (single) illumination, in Fig. 1(c), we show the normalized scattering powers in each channel for a single TM wave excitation along x axis. As one can see from the left panel in Fig. 1(c), the dominant channels are a_{-1}^{TM} and a_1^{TM} [21]. At the same time, the corresponding intensity of total magnetic field in the right panel in Fig. 1(c) reflects the resonant ED.

Now, with multiple coherent waves excitation, suppose we want to eliminate all the lowest channels, i.e., $n = -2$ (EQ), $n = -1$ (ED), $n = 1$ (ED), and $n = 2$ (EQ), but keep only the $n = 0$ (MD) channel. Then, the extrinsic interfering factors for each channel are chosen as $[H_{-2}^{\text{inf}} = 0, H_{-1}^{\text{inf}} = 0, H_1^{\text{inf}} = 0, H_2^{\text{inf}} = 0]$ and $H_0^{\text{inf}} = 1H_{\text{ref}}$. By solving Eq. (5), the corresponding incident wave amplitudes are found: $[H_1 = 0.2H_{\text{ref}}, H_2 = 0.2H_{\text{ref}}, H_3 = 0.2H_{\text{ref}}, H_4 = 0.2H_{\text{ref}}, H_5 = 0.2H_{\text{ref}}]$.

The corresponding result for such a five-waves excitation is revealed in the left panel in Fig. 1(d) for the normalized scattering powers in each channel n, defined as $P_{\text{scat}}^{\text{TM}} k_0 (2\sqrt{\mu_0/\epsilon_0}|H_{\text{ref}}|^2)^{-1}$. With the comparison to the single excitation shown in Fig. 1(c), we can clearly see the zeros in EQ and ED channels in the left panel in Fig. 1(d), as we apply multiple excitations. Right now, the non-zero channel is the $n = 0$ (MD) channel. With the intensity of total magnetic field, shown in the right panel in Fig. 1(d), we have an MD pattern with a_0^{TM} inside the system. As we expect, by extrinsic interferometric waves, one can desirably alter the scattering states.

Moreover, to demonstrate the flexibility in controlling light scattering by our proposed multiple coherent waves excitation, in Fig. 1(e), we demonstrate another setting for the interfering factors by choosing $[H_{-2}^{\text{inf}} = 0, H_{-1}^{\text{inf}} = 1H_{\text{ref}}, H_0^{\text{inf}} = 0, H_1^{\text{inf}} = 0, H_2^{\text{inf}} = 0]$. Even with the same illumination directions given in Fig. 1(b), this set of parameters gives us destructive interferences at $n = -2$, $n = 0$, $n = 1$, and $n = 2$ channels, but with the constructive interference at the $n = -1$ channel. The corresponding incident wave amplitudes are $[H_{-2} = 0.2H_{\text{ref}}, H_{-1} = (0.06 - 0.2i)H_{\text{ref}}, H_0 = (-0.16 - 0.12i)H_{\text{ref}}, H_1 = (-0.16 + 0.12i)H_{\text{ref}}, H_2 = (0.06 + 0.2i)H_{\text{ref}}]$. Here, the ED preserved in $|a_{-1}^{\text{TM}}| = 1$ is displayed in the corresponding intensity plot of the magnetic field.

It is known that the resulting scattering coefficient has a symmetry property when one replaces $n \leftrightarrow -n$. Nevertheless, with a proper set of multiple waves excitation, the symmetry breaking can be achieved as the incident amplitudes become complex. As shown in Fig. 1(e), only a non-zero value is established at the $n = -1$ channel.

Next, we consider the interferometric effect on partial absorption powers. As an illustration, we choose a larger scatterer with the radius $a = 0.2\lambda$, but embedded by a lossy nonmagnetic material $\epsilon_1 = -3 + 0.3i$. As shown in Fig. 2(a), by a single excitation, we can see the multi-channel resonances excited in scattering and absorption powers. Intensity of the total magnetic field is illustrated in the right panel in Fig. 2(a), revealing the maximum strengths around the scatterer. Now, we choose the interfering factors by $[H_{-2}^{\text{inf}} = 0.1H_{\text{ref}}, H_{-1}^{\text{inf}} = 0.5H_{\text{ref}}, H_0^{\text{inf}} = 0, H_1^{\text{inf}} = 0, H_2^{\text{inf}} = 0]$, with the same illumination configuration in Fig. 1(b), with the corresponding incident wave amplitudes being $[H_{-2} = 0.12H_{\text{ref}}, H_{-1} = (0.014 - 0.11i)H_{\text{ref}}, H_0 = (-0.074 - 0.04i)H_{\text{ref}}, H_1 = (-0.074 + 0.04i)H_{\text{ref}}, H_2 = (0.014 + 0.11i)H_{\text{ref}}]$. In this multiple excitation, our strategy is to turn off the channels at $n = 0$ to $n = 2$ and to switch on $n = -2$ and $n = -1$ channels with different weightings. Interestingly, the consequence of this interferometric illumination would lead to maximum absorption occurring at the $n = -1$ channel, as opposed to that at the $n = -2$ channel when encountering single excitation, as shown in Figs. 2(a) and 2(b). The interferometric technology alters the absorption and scattering power distribution at different channels. Our proposed interferometric approach, which

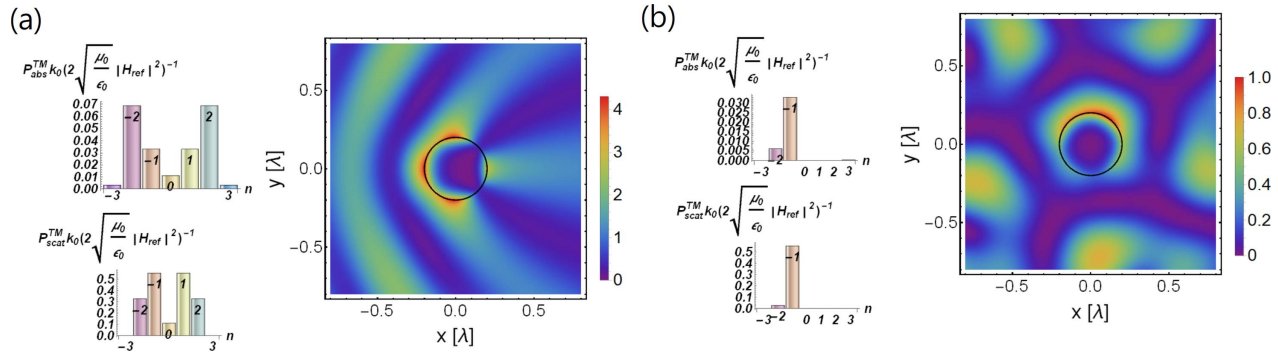

Fig. 2. For a lossy scatter, we show the comparison between (a) single and (b) multiple excitations. The setting configuration of this illumination is the same as that in Fig. 1(b), but with different wave amplitudes. Note that all the field plots are depicted in units of $|H_{\text{ref}}|^2$.

may turn off or turn on the specific channels, is irrespective of inherent systems such as geometry, materials, and structures. We also note that the use of two counter-propagation waves excitation experimentally also demonstrates the changes in scattering modes [22].

In conclusion, based on the interferometric concept, we study the scattering in cylindrical systems upon multiple coherent waves excitation. The scattering and dissipation powers for a cylindrical object encountered by multiple TM waves excitation are rigorously derived for arbitrary irradiation angles, amplitudes, and phases. An interfering factor is introduced to tailor the overall incident, scattering, and internal fields. By manipulating the interfering factors, we not only extrinsically control the scattering and absorption characteristics, but also modulate the targeted channels. With five waves excitation as examples, we demonstrate how systems with different materials and arbitrary sizes can retain the required scattering channels. Moreover, we also create destructive interferences to break the inherently rotational symmetry in the cylindrical scattering coefficients. In general, the solution to support designed scattering channels is not unique, which provides a flexible degree of freedom in a wave interferometric framework. In addition to TM wave excitation, our methodology can be easily extended to TE wave excitation [23] and more complex geometry and structures, which offers a route to non-invasion applications in nano-photonics and meta-devices.

Funding. Ministry of Science and Technology, Taiwan (107-2112-M-259-007-MY3, 105-2628-M-007-003-MY4, MOST108-2119-M-009-003); Australian Research Council; UNSW Scientia Fellowship.

REFERENCES AND NOTES

1. J. D. Jackson, *Classical Electrodynamics* (Wiley, 1975).
2. C. F. Bohren and D. R. Huffman, *Absorption and Scattering of Light by Small Particles* (Wiley, 1983).
3. P. Grahn, A. Shevchenko, and M. Kaivola, New J. Phys. **14**, 093033 (2012).
4. J. A. Schuller, R. Zia, T. Taubner, and M. L. Brongersma, Phys. Rev. Lett. **99**, 107401 (2007).
5. T. Feng, Y. Xu, W. Zhang, and A. E. Miroshnichenko, Phys. Rev. Lett. **118**, 173901 (2017).
6. W. Liu, Phys. Rev. Lett. **119**, 123902 (2017).
7. A. Alú and N. Engheta, Phys. Rev. E **72**, 016623 (2005).
8. J. Y. Lee and R.-K. Lee, Phys. Rev. B **89**, 155425 (2014).
9. S. Arslanagić and R. W. Ziolkowski, Phys. Rev. Lett. **120**, 237401 (2018).
10. H. Noh, Y.-D. Chong, A. D. Stone, and H. Cao, Phys. Rev. Lett. **108**, 186805 (2012).
11. J. Y. Lee and R.-K. Lee, Opt. Express **24**, 6480 (2016).
12. J. Y. Lee, A. E. Miroshnichenko, and R.-K. Lee, Phys. Rev. A **96**, 043846 (2017).
13. J. Y. Lee, A. E. Miroshnichenko, and R.-K. Lee, Opt. Express **26**, 30393 (2018).
14. A. E. Miroshnichenko, A. B. Evlyukhin, Y. F. Yu, R. M. Bakker, A. Chipouline, A. I. Kuznetsov, B. Lukýanchuk, B. N. Chichkov, and Y. S. Kivshar, Nat. Commun. **6**, 8069 (2015).
15. Z. Ruan and S.-H. Fan, Phys. Rev. Lett. **105**, 013901 (2010).
16. T. Das, P. P. Iyer, R. A. DeCrescent, and J. A. Schuller, Phys. Rev. B **92**, 241110(R) (2015).
17. Z. Xi and H. P. Urbach, Phys. Rev. Lett. **119**, 053902 (2017).
18. A. Bag, M. Neugebauer, P. Woźniak, G. Leuchs, and P. Banzer, Phys. Rev. Lett. **121**, 193902 (2018).
19. L. Wei, A. V. Zayats, and F. J. Rodriguez-Fortuño, Phys. Rev. Lett. **121**, 193901 (2018).
20. G. J. Gbur, *Mathematical Methods for Optical Physics and Engineering* (Cambridge University, 2011).
21. Although this system possesses the electric dipole resonant, there are still extremely small residual strengths in the other channels. In particular, we find $|a_0^{TE}| = 0.002$.
22. X. Fang, M. L. Tseng, D. P. Tsai, and N. I. Zheludev, Phys. Rev. Appl. **5**, 014010 (2016).
23. Due to electromagnetic duality, the related formulas could be obtained by replacing $\epsilon \to \mu$, $\mu \to \varepsilon$, $\vec{E} \to \vec{H}$, and $\vec{H} \to -\vec{E}$.